the plant journal

SEB Society for Experimental Biology

The Plant Journal (2013) **74,** 226–238 doi: 10.1111/tpj.12115

Identification of rice *Allene Oxide Cyclase* mutants and the function of jasmonate for defence against *Magnaporthe oryzae*

Michael Riemann[1,2,†], Ken Haga[3,†,‡], Takafumi Shimizu[4,†,§], Kazunori Okada[4], Sugihiro Ando[2,¶], Susumu Mochizuki[2], Yoko Nishizawa[2], Utako Yamanouchi[5], Peter Nick[1], Masahiro Yano[6], Eiichi Minami[2], Makoto Takano[2], Hisakazu Yamane[4,7] and Moritoshi Iino[3,*]

[1]*Botanical Institute, Molecular Cell Biology, Karlsruhe Institute of Technology, Kaiserstraße 2, 76131 Karlsruhe, Germany,*
[2]*Division of Plant Sciences, National Institute of Agrobiological Sciences, 2–1–2 Kannondai, Tsukuba, Ibaraki 305–8602, Japan,*
[3]*Botanical Gardens, Graduate School of Science, Osaka City University, Kisaichi, Katano-shi, Osaka 576–0004, Japan,*
[4]*Biotechnology Research Center, University of Tokyo, 1–1–1 Yayoi, Bunkyo–ku, Tokyo 113–8657, Japan,*
[5]*Rice Applied Genomics Research Unit, National Institute of Agrobiological Sciences, 2–1–2 Kannondai, Tsukuba, Ibaraki 305–8602, Japan,*
[6]*Agrigenomics Research Center, National Institute of Agrobiological Sciences, 1–2 Ohwashi, Tsukuba, Ibaraki 305–8634, Japan, and*
[7]*Department of Biosciences, Teikyo University, 1–1 Toyosatodai, Utsunomiya 320–8551, Japan*

Received 16 November 2012; revised 17 December 2012; accepted 2 January 2013; published online 24 January 2013.
*For correspondence (e-mail iino@sci.osaka-cu.ac.jp).
†These authors contributed equally to this work.
‡Present address: Graduate School of Science and Technology, Niigata University, Nishi–ku, Niigata 950–2181, Japan.
§Present address: Botanical Gardens, Graduate School of Science, Osaka City University, Kisaichi, Katano–shi, Osaka 576–0004, Japan.
¶ Present address: Graduate School of Agricultural Science, Tohoku University, 1–1 Amamiya-machi, Tsutsumidori, Aoba–ku, Sendai, Miyagi 981–8555, Japan.

SUMMARY

Two photomorphogenic mutants of rice, *coleoptile photomorphogenesis 2* (*cpm2*) and *hebiba*, were found to be defective in the gene encoding allene oxide cyclase (*OsAOC*) by map-based cloning and complementation assays. Examination of the enzymatic activity of recombinant GST–OsAOC indicated that OsAOC is a functional enzyme that is involved in the biosynthesis of jasmonic acid and related compounds. The level of jasmonate was extremely low in both mutants, in agreement with the fact that rice has only one gene encoding allene oxide cyclase. Several flower-related mutant phenotypes were observed, including morphological abnormalities of the flower and early flowering. We used these mutants to investigate the function of jasmonate in the defence response to the blast fungus *Magnaporthe oryzae*. Inoculation assays with fungal spores revealed that both mutants are more susceptible than wild-type to an incompatible strain of *M. oryzae*, in such a way that hyphal growth was enhanced in mutant tissues. The level of jasmonate isoleucine, a bioactive form of jasmonate, increased in response to blast infection. Furthermore, blast-induced accumulation of phytoalexins, especially that of the flavonoid sakuranetin, was found to be severely impaired in *cpm2* and *hebiba*. Together, the present study demonstrates that, in rice, jasmonate mediates the defence response against blast fungus.

Keywords: jasmonate, blast disease, *Oryza sativa*, *Magnaporthe oryzae*, phytoalexin, sterility.

INTRODUCTION

An increasing body of evidence supports a major role of jasmonates [jasmonic acid (JA) and related compounds] as a hormone in plant development and in plant responses to environment. For instance, the role of jasmonate in wound signalling has been characterized in great detail (Koo and Howe, 2009). In some plant species, jasmonate has been shown to function in developmental processes such as anther dehiscence (Ishiguro *et al.*, 2001), tendril coiling (Falkenstein *et al.*, 1991) and sex determination (Acosta *et al.*, 2009; Yan *et al.*, 2012). Jasmonate is an important

regulator of plant defence against abiotic and biotic stresses, and is involved in the induction of cell death (Reinbothe *et al.*, 2009). Furthermore, a function of jasmonate in photomorphogenesis has been found, which is described below in more detail.

Jasmonate is biosynthesized from linolenic acid in a canonical pathway (Vick and Zimmerman, 1984; Wasternack, 2007) involving several cell compartments and enzymes: allene oxide synthase (AOS) catalyses the formation of an unstable allene oxide, which is converted exclusively by allene oxide cyclase (AOC) to the naturally occurring enantiomer of 12–oxo-phytodienoic acid (OPDA), leading to formation of the naturally occurring enantiomer of JA. As allene oxide, the product of AOS, is not stable, it is non-enzymatically converted to racemic OPDA in the absence of AOC (Hamberg and Fahlstadius, 1990).

The identification of CORONATINE INSENSITIVE 1 (COI1) as a JA receptor revealed that it is not free JA, but rather its conjugate with the amino acid isoleucine (JA–Ile), that is the bioactive form of JA. COI1, an F–box protein that forms an SCF complex together with ASK1 (an SKP1 homologue) and CULLIN1, recruits JAZ proteins into a complex. These proteins, repressors of the jasmonate response, are marked for degradation via the 26S proteasome pathway (Xie *et al.*, 1998; Chini *et al.*, 2007; Thines *et al.*, 2007; Yang *et al.*, 2012). The conjugation of JA to Ile is catalysed by a GH3 enzyme called JASMONATE RESISTANT 1 (JAR1) (Staswick and Tiryaki, 2004; Staswick, 2008).

Previously, we isolated the rice (*Oryza sativa* L.) mutants *coleoptile photomorphogenesis 1* (*cpm1*; Biswas *et al.*, 2003) and *hebiba* (Riemann *et al.*, 2003), which are impaired in seedling photomorphogenesis. Subsequent studies indicated that biosynthesis of JA and transcription of a rice *AOS* gene and JA response genes are regulated by phytochrome (Haga and Iino, 2004; Riemann *et al.*, 2007, 2008). Furthermore, the degradation of photoactivated phytochrome A in the dark was shown to be delayed in *hebiba* coleoptiles (Riemann *et al.*, 2009). These results suggest that jasmonate is involved in phytochrome-mediated photomorphogenesis of rice seedlings. Jasmonate biosynthesis mutants of Arabidopsis are partially impaired in growth responses to far-red (FR) light, suggesting that jasmonate is also involved in photomorphogenesis of Arabidopsis seedlings (Hsieh *et al.*, 2000; Chen *et al.*, 2007; Robson *et al.*, 2010).

Jasmonate has been suggested to participate in the defence response to the fungal pathogen *Magnaporthe oryzae*. This possibility is supported by the observation that a chemical inducer of blast resistance, 2,6–dichloroisonicotinic acid (INA), may induce JA and JA-dependent transcripts (Schweizer *et al.*, 1997). Phytoalexins are important antimicrobial secondary metabolites that are produced in response to pathogen infection. Several phytoalexins have been shown to accumulate upon blast inoculation (Kodama *et al.*, 1992; Dillon *et al.*, 1997; Grayer and Kokubun, 2001), and the synthesis of several phytoalexins has been shown to be induced by exogenous JA (Rakwal *et al.*, 1996).

The analysis of jasmonate function in the response to fungal infection was limited by the fact that well-characterized JA-deficient mutants were not available. The mutant *hebiba* was found to be deficient in JA, but the causative mutation was not known (Riemann *et al.*, 2003). We isolated another mutant, *cpm2*, showing phenotypes very similar to that of *hebiba*. In the present work, we found that *AOC* is responsible for the overlapping phenotypes of the two mutants. Subsequently, we made use of these mutants to investigate the function of jasmonate in the defence against fungal pathogens using *M. oryzae* as a model.

RESULTS

Isolation of the *cpm2* mutant and its comparison with *hebiba*

The *cpm2* mutant was isolated from a γ–ray-mutagenized M_2 population of *japonica* rice (cv. Nihonmasari) based on a long-coleoptile phenotype under continuous white light (Biswas *et al.*, 2003). In addition, the mutant exhibited a long mesocotyl in etiolated seedlings. Furthermore, the mutant produced at most only a few fertile seeds in each panicle and is almost sterile. As the mutant was successfully pollinated by the wild-type, this feature is apparently caused by a reduction in male fertility.

All of these traits have been observed in the mutant *hebiba* (Riemann *et al.*, 2003). Hence we compared the two mutants under identical conditions to quantify their long-coleoptile phenotype. Because it was difficult to obtain homozygous mutant seeds in sufficient quantity due to male sterility, the experiments were performed using heterozygous populations. Seedlings were raised under continuous red light for several days until the first leaf emerged from the coleoptile to determine their final coleoptile length. Within heterozygous populations of the two mutants, a 3:1 segregation pattern characteristic of a recessive mutation was observed: a quarter of the plants showed long coleoptiles (*cpm2* 27.9%, *hebiba* 23.2%), while the other plants showed short coleoptiles similar to the wild-type Nihonmasari (Figure 1). The wild-type had a mean final coleoptile length of 6.6 mm, but *cpm2* and *hebiba* developed significantly longer coleoptiles (16.0 and 23.4 mm for *cpm2* and *hebiba*, respectively). Thus, both mutants exhibit the long-coleoptile phenotype, but with different amplitude.

Identification of *CPM2* and *HEBIBA* loci by map-based analysis

We used a map-based cloning strategy to identify the mutations responsible for the *cpm2* and *hebiba* phenotypes.

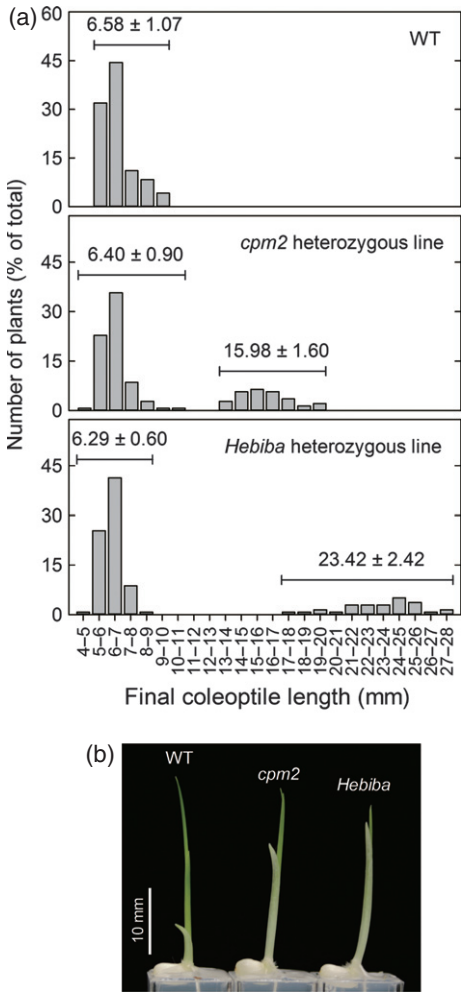

Figure 1. Long-coleoptile phenotype of *cpm2* and *hebiba* mutants.
(a) Distribution of the final coleoptile length under continuous red light in the wild-type (n = 72), *cpm2* heterozygous line (n = 140) and *hebiba* heterozygous line (n = 138). Values are the number of seedlings (percentage of the total examined) in each length division (1 mm intervals). The numbers indicate the mean ± SD final coleoptile length determined for the short-coleoptile and long-coleoptile groups of seedlings (indicated by horizontal bars).
(b) Wild-type, *cpm2* and *hebiba* seedlings. The photographs for *cpm2* and *hebiba* represent the long-coleoptile groups in (a).

The *cpm2* mutant was crossed with the *indica* cultivar Habataki, which showed a final coleoptile length similar to that of Nihonmasari (Figure S1). Approximately 4000 F_2 seedlings were screened for a long-coleoptile phenotype under continuous red light. Selected seedlings (738) were transferred to soil and raised further. Part of the second leaf was harvested from each plant, frozen, and subjected to DNA extraction. The DNA samples were used for subsequent analysis. We were able to confirm sterility in all of the plants grown to maturity.

After rough mapping using a DNA sample from ten individuals, the mutation was found to be located on chromosome 3 between the SSR markers RM15224 and RM3513 (Table S1). Subsequently, DNA samples of all individuals were used for fine mapping analysis, and the identified region containing the *CPM2* locus was narrowed to between the SSR markers AC114896–1 and AC093312–1, which are located close to the publicly available markers RM15253 and RM15326, respectively (Figure 2a and Table S1). The marked region encompassed approximately 2.8 Mbp. We attempted to narrow the candidate region further without a success due to the highly repetitive sequences found between markers AC097367a and AC093312–1. Furthermore, the recombination rate around the mapped region was apparently very low, probably due to the presence of the centromere between the markers AC106887–1 and RM15326.

By analysing individuals of a *hebiba* x Kasalath population displaying a clear long-coleoptile phenotype, we found that some SSR markers within the *CPM2* candidate region (AC106887–1, AC147803d and AC0907367a, Figure 2a and Table S1) could not be amplified, suggesting that *hebiba* has a genomic deletion in the region containing these markers. We determined the sequences flanking the deletion by inverse PCR using genomic DNA of *hebiba* as a template, and found a deletion of approximately 170 kb (Figure 2a). The same deletion was identified by a novel sequencing method independently of us (Nordström *et al.*, 2013).

Within the deleted region, the gene *OsAOC* [Os03 g0438100 according to the Rice Annotation Project database (http://rapdb.dna.affrc.go.jp/); LOC_Os03 g32314.1 according to the Michigan State University Rice Genome Annotation Project (http://rice.plantbiology.msu.edu/)], which encodes a key enzyme for JA biosynthesis, was identified. We sequenced *OsAOC* of *cpm2* and detected a deletion of 11 bp in the first exon of this gene (Figure 2b). Therefore, *OsAOC* appears to be the most likely candidate gene causing the common phenotypes of the two mutants.

Complementation of *cpm2* and *hebiba* by *OsAOC*

Based on the above analysis, the *cpm2* mutant was transformed with a genomic fragment containing the *OsAOC* promoter and the coding region. The T_1 generation of complemented *cpm2* plants was raised under continuous red light to determine the final coleoptile length. Approximately three-quarters of T_1 seedlings had short coleoptiles comparable to those of wild-type, indicating that *cpm2* was complemented by *OsAOC*. Some T_1 seedlings were grown to maturity to harvest T_2 caryopses. From those caryopses, we obtained homozygous T_2 populations, all individuals of which carry the transgene and show the wild-type phenotype with regard to the final coleoptile length (Figure 3a,b). Furthermore, it was found that the T_1 plants determined to be homozygous transformants show a wild-type level of fertility, demonstrating that the sterility of the mutant was also rescued by the

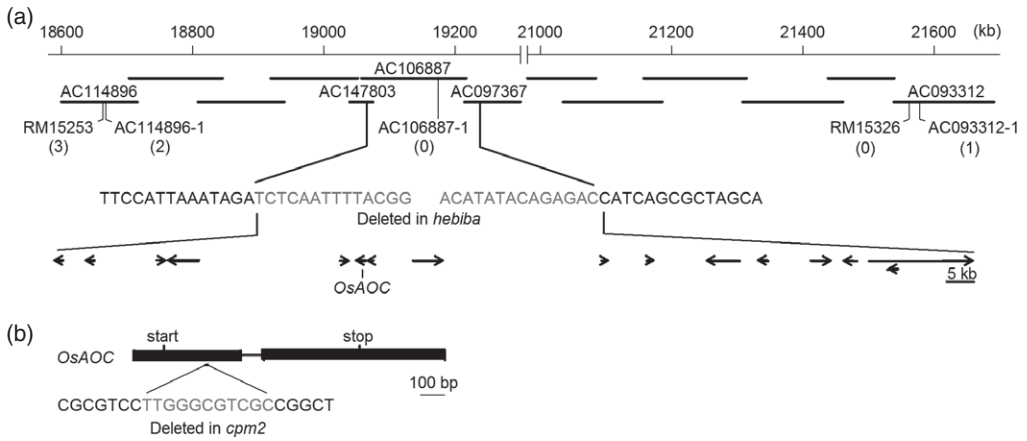

Figure 2. Map-based analysis of the genomic loci responsible for *cpm2* and *hebiba* mutations.
(a) A region of chromosome 3 in which *cpm2* and *hebiba* were found to be mutated. Map-based analysis indicated that the locus responsible for the *cpm2* mutation resides between the markers AC114896–1 and AC093312–1. Within this region, *hebiba* was found to have a deletion of 170 kb that contains the rice allene oxide cyclase gene (*OsAOC*). The border sequences of the deleted region are shown; sequences in grey indicate the deleted edges. Black bars represent BAC clones. The numbers in parentheses indicate the number of recombinants. Horizontal arrows indicate the positions of genes annotated by the Rice Annotation Project database (http://rapdb.dna.affrc.go.jp/).
(b) Mutation of *OsAOC* found in *cpm2*. The first exon was found to have a deletion of 11 bp, which is shown in grey.

transgene (Figure 3c). We also transformed the *hebiba* mutant with a genomic fragment containing the *OsAOC* promoter and coding region. As shown in Figure 3(d), approximately three-quarters of the T_1 seedlings had short coleoptiles comparable to wild-type coleoptiles. The plants with short coleoptiles were determined to be transgenic, while those with a long coleoptile were not. Thus, *hebiba* was also complemented by *OsAOC*. From

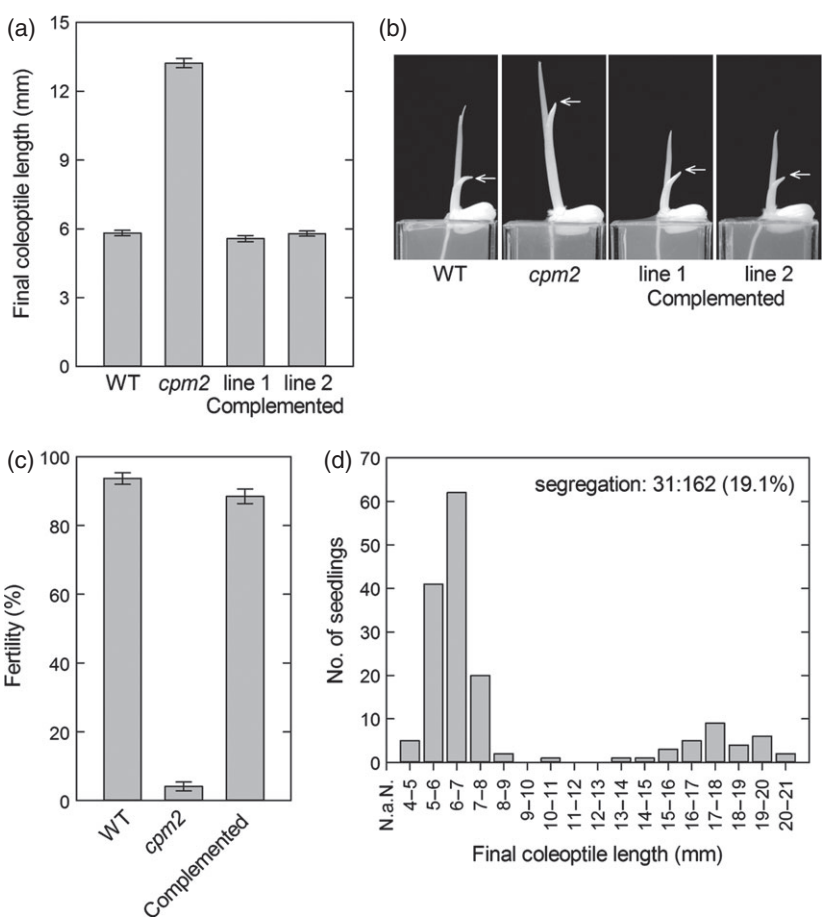

Figure 3. Complementation of *cpm2* and *hebiba* mutants.
(a) Final coleoptile length in seedlings of the wild-type (WT), *cpm2* and two complemented *cpm2* lines (T_2 generation) raised under continuous red light. Values are means ± SE of 19-34 seedlings.
(b) Representative seedlings of WT, *cpm2* and two complemented *cpm2* lines raised as described above. The arrows indicate the tips of the coleoptiles.
(c) Fertility of wild-type (WT), *cpm2* and complemented *cpm2* plants. The complemented plans used were of the T_1 generation, and were determined to be homozygous transformants by analysis of T_2 seedlings.
(d) Distribution of the final coleoptile length in complemented *habiba* seedlings (T_1 generation) raised under continuous red light. A total of 162 caryopses harvested from four independent T_0 transformants were used to obtain the data.

these results, we conclude that the lack of functional *OsAOC* is responsible for the common mutant phenotypes in *cpm2* and *hebiba*.

OsAOC encodes a functional AOC

In order to verify the presumed AOC activity of the product encoded by *OsAOC*, we used a recombinantly expressed GST fusion protein in combination with recombinantly expressed GST–OsAOS1, as described by Stenzel *et al.* (2003) and Zerbe *et al.* (2007), to perform a coupled enzyme assay. OsAOS1 was confirmed to be a functional AOS by a spectrophotometric enzyme assay (K.H. and M.I., unpublished results). Both proteins were expressed without the chloroplast target signal. After purification by affinity chromatography (Figure S2), protein samples were subjected to an enzyme activity assay. The substrate of AOS, 13–hydroperoxy-octadecatrienoic acid (13–HPOT), was metabolized, presumably into allene oxide, when GST–OsAOS1 was present in the reaction mixture, but remained unaltered in the absence of GST–OsAOS1 (Figure 4a). In the presence of both GST–AOS1 and GST–OsAOC, *cis*-(+)-OPDA was preferentially synthesized. This OPDA enantiomer is the precursor of the naturally occurring JA (Stintzi *et al.*, 2001; Taki *et al.*, 2005; Bottcher and Pollmann, 2009). In the presence of GST–OsAOS1 only, racemic OPDA was produced (Figure 4b and Figure S3), and no OPDA (not even in racemic form) was detectable when only GST–OsAOC or neither of the two enzymes was present in the reaction mixture (Figure 4b). This result indicates that *OsAOC* encodes a functional AOC.

Jasmonate levels are severely reduced in *cpm2* and *hebiba*

In order to test whether *OsAOC* is required for the biosynthesis of jasmonate, we compared endogenous levels of JA and JA–Ile in the fourth leaf sheaths of 3-week-old plants of the wild-type, *cpm2* and *hebiba.* JA and JA–Ile were extracted from the plant materials and quantified by HPLC-ESI-MS/MS using a chiral column that enabled the separation of natural and unnatural enantiomers of JA. Endogenous levels of natural JA in the wild-type, *cpm2* and *hebiba* were 6.0, 0.5 and 0.5 ng g^{-1} fresh weight (FW) (Figure 5a,c), and those of natural JA–Ile were 0.5, 0.03 and 0.05 ng g^{-1} FW, respectively (Figure 5b,d), demonstrating that jasmonate biosynthesis is severely suppressed in *cpm2* and *hebiba*. A low level of natural JA (approximately one-tenth of the wild-type) was detected in both *cpm2* and *hebiba*. A comparable level of unnatural JA was also detected in the two mutants, but was not detected at all in the wild-type (Figure 5a,c). These results indicate that the wild-type exclusively biosynthesizes the natural JA enantiomer, whereas the mutants produce low levels of racemic JA from allene oxide, most probably in a non-enzymatic manner.

As it has been well established that jasmonate biosynthesis is transiently induced by wounding in rice leaf blades (Kiribuchi *et al.*, 2005), we compared the levels of JA and JA–Ile in wounded leaf blades of the wild-type, *cpm2* and *hebiba*. In the wild-type, accumulation of JA and JA–Ile was initiated within 30 min, peaking at 1 h (JA, 379 ng g^{-1} FW) or 30 min (JA–Ile, 107 ng g^{-1} FW) after wounding (Figure S4). Such wound-induced accumulation of JA and JA–Ile was undetectable in *cpm2* and *hebiba*, confirming that JA biosynthesis does not operate in the mutants.

Altered flower morphology and heading time in JA biosynthesis mutants

Abnormal anthesis was observed in *cpm1*, a mutant of *OsAOS1* (Haga and Iino, 2004), but the overall flower morphology remained unaltered (Figure 6a) (Biswas *et al.*, 2003). In contrast, *cpm2* and *hebiba* flowers showed clear morphological differences from wild-type flowers. The

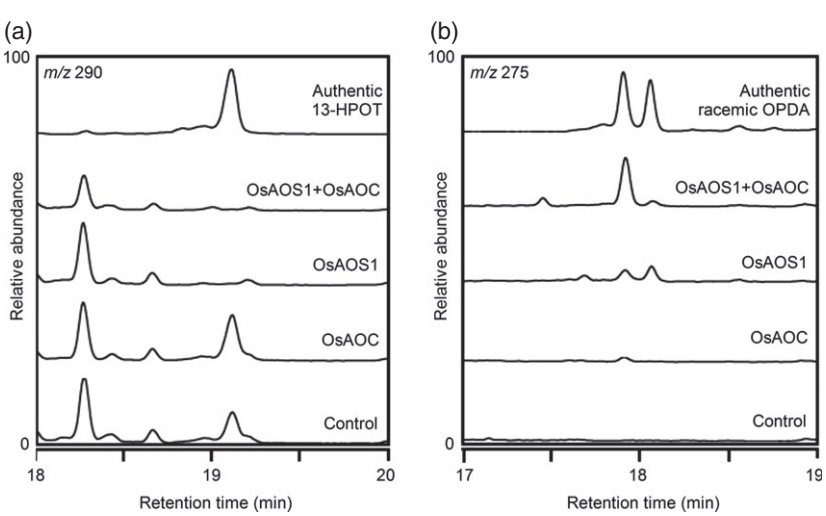

Figure 4. Enzymatic activity of OsAOC.
Chiral GC–MS analysis of reaction products catalysed by OsAOS1, OsAOC, and OsAOS1 plus OsAOC in the same reaction mix. The data show a representative result from a series of three experiments.
(a) Mass chromatograms of the selected ion (*m/z* 290) for 13–HPOT. The chromatogram for authentic 13–HPOT is shown at the top. The reaction mixture contained both GST–OsAOS1 and GST–OsAOC (OsAOS1 + OsAOC), only GST–OsAOS1 (OsAOS1), only GST–OsAOC (OsAOC), or no protein preparation (control).
(b) Mass chromatograms of the selected ion (*m/z* 275) for racemic OPDA. The chromatogram for authentic racemic OPDA is shown at the top. The reaction conditions were as described for (a).

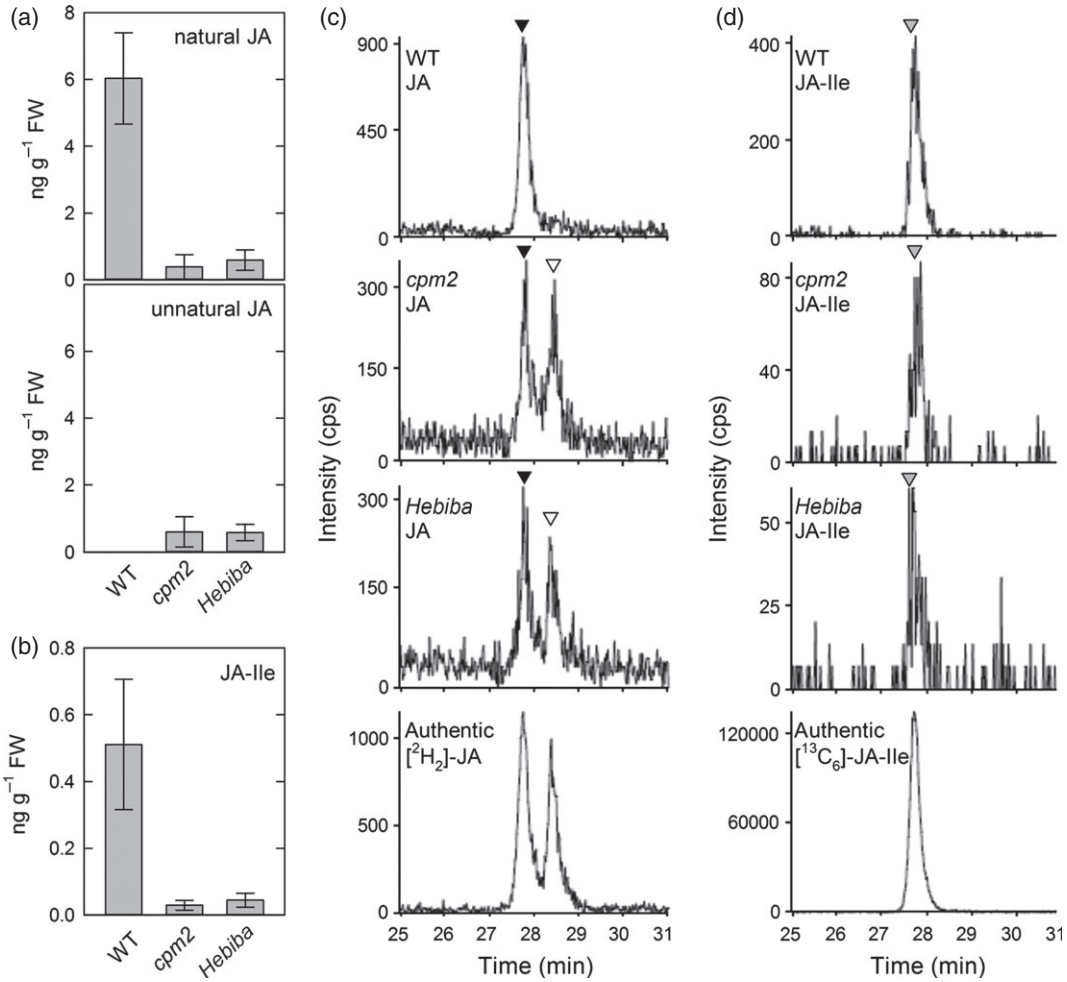

Figure 5. Deficiency of jasmonate in *cpm2* and *hebiba*.
(a,b) Levels of natural and unnatural JA (a) and JA–Ile (b) in the fourth leaf sheaths of the wild-type, *cpm2* and *hebiba*. Twenty-one—day-old plants were used. Values are means ± SE of three independent samples.
(c,d) Examples of MS/MS chromatograms used for analysis. Chromatograms were obtained at *m/z* 209/59 (JA), *m/z* 211/59 ([2H2]-JA), *m/z* 322/130 (JA–Ile) and *m/z* 328/130 ([$^{13}C_6$]-JA–Ile). Black and white arrowheads indicate peaks of natural and unnatural JA, respectively. Grey arrowheads indicate peaks of JA–Ile.

sterile lemmas of most mutant flowers were longer compared to the wild-type flowers, and some mutant flowers showed an elongated palea (Figure 6a and Figure S5) (see Yoshida and Nagato, 2011; for rice flower morphology). Occasionally additional bract-like organs developed in the mutants between the sterile lemma and palea (Figure 6a, indicated by arrows), or between the lemma and palea, as well as additional anthers (up to seven) and pistils (up to three).

Previously, *hebiba* was found to show early heading (Riemann *et al.*, 2003). We therefore compared heading times of the wild-type, *cpm1 cpm2* and *hebiba* under short-day conditions (10 h light/14 h darkness, Figure 6b). Under these conditions, the inflorescences of wild-type plants appeared after 50 days. This period was significantly shorter in all tested mutants (*cpm1*, 45.8 days; *cpm2*, 44.7 days; *hebiba*, 42.5 days). Even under long-day conditions, *cpm2* and *hebiba* showed significantly earlier heading.

Jasmonate is required for defence against *M. oryzae*

We used *cpm2* and *hebiba* to investigate a possible involvement of jasmonate in the resistance to fungal pathogens. Excised leaf sheaths were inoculated with spores of *M. oryzae*, and the growth of *M. oryzae* hyphae in the epidermis was investigated microscopically. The experiments were performed in the absence or presence of exogenous JA. The extent of infection was separated into three categories: 'infected' (more than one cell was infected with hyphae originating from the observed appressorium), 'one cell infected' (only one cell beneath the observed appressorium was infected by hyphae), or 'non-infected' (no cell was infected by the observed appressorium) (Figure 7a). We first compared the susceptibility to a compatible strain (Ina86–137) between the wild-type and *cpm2*, but found no significant difference (Figure S6a). However, application of JA caused a significant reduction in susceptibility (a

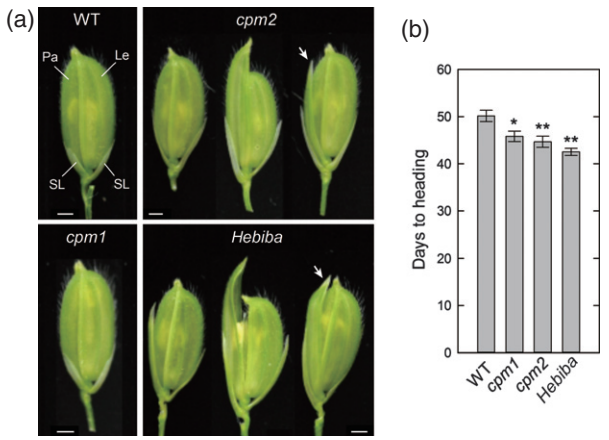

Figure 6. Altered flower morphology and heading time in jasmonate-deficient rice mutants.
(a) Flower shape in the wild-type and *cpm1*, *cpm2* and *hebiba* mutants. The *cpm1* flower has elongated filaments, that are not apparent in the photograph (Biswas *et al.*, 2003). The *cpm2* and hebiba flowers develop elongated sterile lemma (SL), and, in some cases, elongated palea (Pa), while the lemma (Le) showed the same morphology as the wild type. Some *cpm2* and *hebiba* flowers develop an additional organ between Pa and SL (indicated by arrows). Scale bars = 10 mm.
(b) Heading time in the wild-type and *cpm1*, *cpm2* and *hebiba* mutants under short-day conditions (10 h light/14 h dark). Values are means ± SE of six plants. Asterisks indicate statistically significant differences from the wild-type (Student's *t* test; $*P < 0.05$ and $**P < 0.01$).

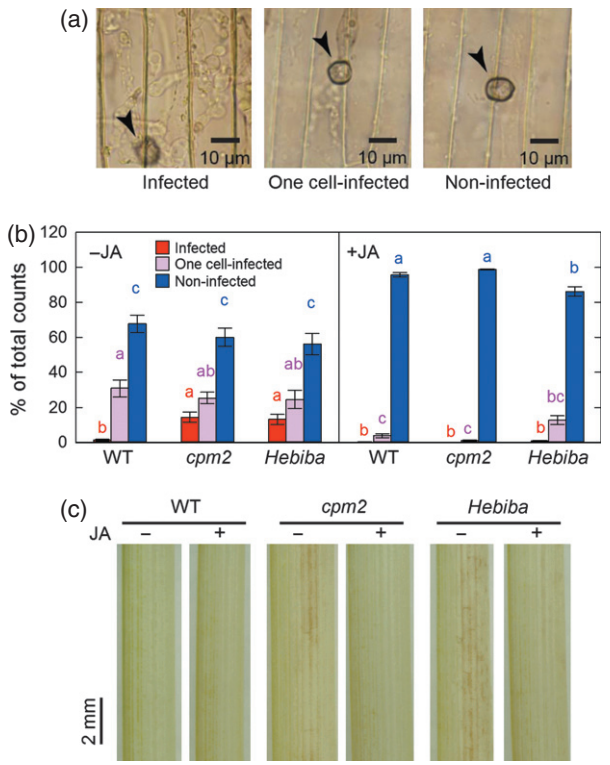

Figure 7. *Magnaporthe oryzae* (P91–15B) inoculation assay using excised leaf sheaths of the wild-type, *cpm2* and *hebiba*.
(a) Various categories of hyphal infection. The photographs represent the three categories of infection defined with regard to the hyphal development observed from each appressorium. Arrowheads indicate fungal appressoria.
(b) Proportions of the various infection categories in wild-type, *cpm2* and *hebiba* leaf sheaths. The assay was performed with or without applied JA (100 μM). Values are means ± SE obtained from eight or nine leaf sheaths, with 75–400 appressoria counted in each leaf sheath. The data for each infection category, including those obtained with and without applied JA, were analysed statistically by Tukey's test. Different letters indicate significant differences at $P < 0.05$.
(c) Leaf sheaths of the wild-type, *cpm2* and *hebiba* infected with *M. oryzae* with or without applied JA. Typical examples obtained at 2 dpi are shown. Note the tissue browning that developed in *cpm2* and *hebiba*, but not in the wild-type. This browning did not occur in the presence of applied JA.

decrease in the proportion of cells in the 'infected' and 'one cell infected' categories) in the wild-type (Figure S6b).

We performed subsequent experiments with an incompatible strain (P91–15B). In the wild-type control in the absence of exogenous JA, the proportion of the appressoria causing the category 'infected' category was 1.4%, whereas the corresponding proportions in *cpm2* and *hebiba* were 14.6% and 13.3%, respectively (Figure 7b, –JA). The results indicated that resistance against hyphal growth is reduced in jasmonate-deficient mutants. In the presence of exogenous JA, the proportion of appressoria causing the 'infected' category was significantly lower in *cpm2* and *hebiba* compared to that without JA (Figure 7b, +JA). In all three genotypes, treatment with JA reduced the proportion of the appressoria causing the categories 'infected' and 'one cell-infected' categories below that for the control without exogenous JA. These observations indicate that exogenous JA rescues the resistance of the mutants, and that resistance is enhanced in the wild-type by application of JA. Together these results demonstrate that jasmonate plays a significant role in the resistance to fungal infection.

We additionally observed that infected leaf sheaths of the mutants develop tissue browning, indicating accumulation of brownish substances. This tissue browning was probably caused by fungal infection, as reported previously for pathogen-treated rice (Chi *et al.*, 2009), and *Sorghum bicolor* (Nicholson *et al.*, 1987). Tissue browning was not observed in the wild-type; furthermore, the tissue browning observed in the mutants was reduced by JA application (Figure 7c). Our result provides genetic and physiological evidence that the blast-induced tissue browning was caused by the lack of jasmonate.

Subsequently, we examined the effect of *M. oryzae* infection on accumulation of jasmonate levels in the wild-type, and compared them to the levels in mock-treated plants. The levels of JA and its active form JA–Ile in the fourth leaf sheaths were quantified at the time of inoculation (initial), and 1 and 2 days post-inoculation (dpi). Fungal infection did not have an effect on the level of JA. On the other hand, the level of JA–Ile was significantly enhanced by inoculation, and this increase did not occur in

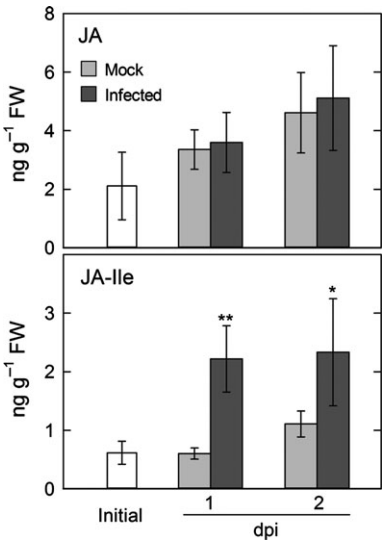

Figure 8. Effects of fungal inoculation on jasmonate levels in rice leaf sheaths.
Excised fourth leaf sheaths of the wild-type were inoculated with P91–15B spores, and the levels of JA and JA–Ile were determined. Values are means ± SE of six independent samples (ten leaf sheath segments/sample) obtained on two occasions (three samples/occasion). Asterisks indicate a statistically significant difference from the mock control (Student's t test, $^{**}P < 0.01$) or a statistically significant difference in the levels of JA–Ile of infected leaf sheaths at 1 and 2 dpi compared with the initial level ($^{*}P < 0.05$).

the mock-treated control (Figure 8). The result indicated that JA–Ile is related to disease resistance.

Jasmonate-dependent production of phytoalexins upon *M. oryzae* infection

Phytoalexins are produced in response to pathogen infection. We investigated the effect of *M. oryzae* infection on production of the flavonoid phytoalexin sakuranetin and the major diterpenoid phytoalexins momilactones and phytocassanes.

As shown in Figure 9(a), the level of sakuranetin was increased at 1 and 2 dpi (with a maximum of 2.5 μg g^{-1} FW at 2 dpi) in the wild-type, but no significant increase was detected in the mutants. However, blast-induced accumulation was observed for momilactones and phytocassanes. Momilactones accumulated to a concentration of 4.3 μg g^{-1} FW at 2 dpi in the wild-type. This response was partially suppressed in *cpm2* and *hebiba*, in which momilactone levels reached 2.4 and 1.6 μg g^{-1} FW at 2 dpi, respectively (Figure 9b and Figure S7). For the pathogen-induced increase of phytocassanes, no significant differences were observed among the wild-type, *cpm2* and *hebiba* (Figure 9c and Figure S7). These results demonstrate that the pathogen-induced accumulation of sakuranetin, and partially that of momilactones, is mediated by jasmonate, but jasmonate is dispensable for synthesis of phytocassanes.

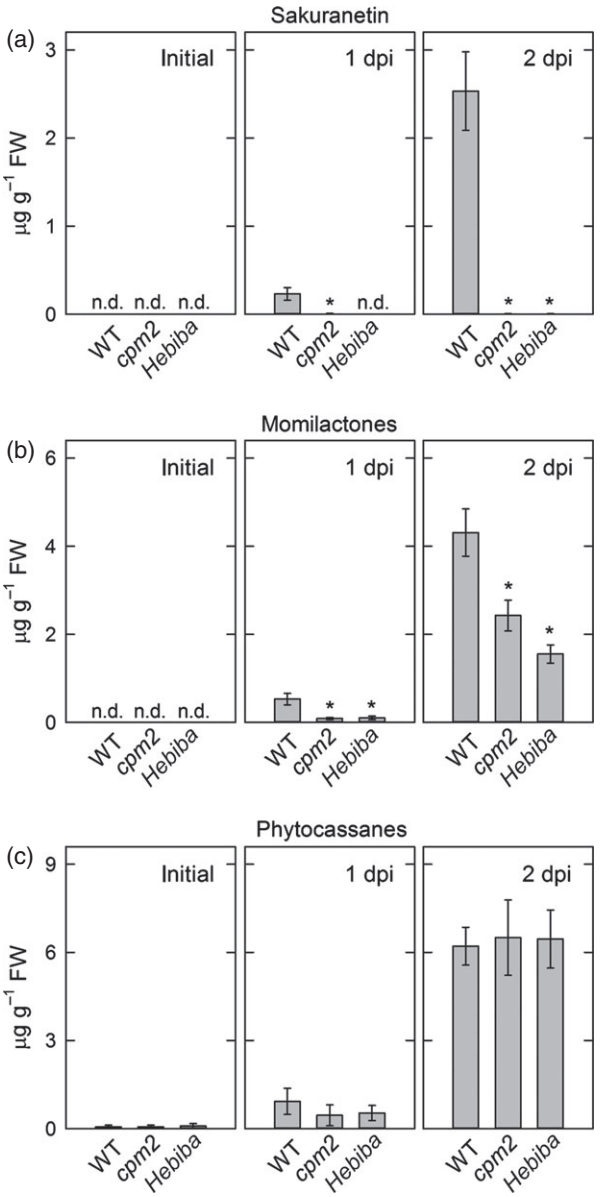

Figure 9. Effects of *Magnaporthe oryzae* (P91–15B) inoculation on the levels of phytoalexins in wild-type, *cpm2* and *hebiba* leaf sheaths.
The levels of sakuranetin (a) momilactones (b) and phytocassanes (c) were determined before infection (initial) and at 1 and 2 dpi. Values are means ± SE of three independent samples. Asterisks indicate statistically significant differences from the wild-type control (Student's *t* test, $^{*}P < 0.05$).

DISCUSSION

Severe jasmonate deficiency in rice *AOC* mutants impairs development

Research on jasmonate biosynthesis and signalling in rice has been limited by the fact that well-characterized biosynthetic mutants were unavailable. We succeeded in isolating two jasmonate-deficient mutants, *cpm2* and *hebiba*. In this study, we demonstrate that mutations in *OsAOC*, which

encodes a key enzyme of JA biosynthesis, are responsible for the phenotypes of *cpm2* and *hebiba*. *OsAOC* is a single-copy gene, which explains the severe jasmonate deficiency of the mutants. This is in contrast to Arabidopsis, which has four copies of *AOC* (Stenzel *et al.*, 2003). Thus the mutants are excellent tools to study the function of jasmonate in rice.

In addition to the photomorphogenic phenotype of seedlings (Figure 1) (Riemann *et al.*, 2003), the two mutants showed developmental phenotypes such as reduced fertility, early flowering and altered flower architecture (Figures 3c and 6, and Figure S5). We confirmed that the open-husk phenotype, as described for *osjar1* mutants (Riemann *et al.*, 2008), is a jasmonate-dependent phenotype. It will be interesting to investigate the role of jasmonate in husk closure in relation to genes such as *OsCRINKLY4* (Pu *et al.*, 2012) that have been shown to participate in this process. We further observed other abnormalities in the morphology of rice flowers that have not been described elsewhere, such as elongated sterile lemma (Figure 6a). In addition, we observed an early-flowering phenotype of the jasmonate-deficient mutants (Figure 6b).

In rice, phytochrome B regulates expression of the florigen Hd3a (Tamaki *et al.*, 2007) via *Heading date 1* (Ishikawa *et al.*, 2011), and it has been shown that phytochrome-deficient mutants show an early-flowering phenotype (Izawa *et al.*, 2002; Takano *et al.*, 2005). Under short-day conditions, *phyB* mutants flowered approximately 10 days earlier compared to the wild-type (Takano *et al.*, 2005). Under similar short-day conditions, the jasmonate-deficient mutants flowered 5-8 days earlier than the wild-type. Because jasmonate biosynthesis is likely to be regulated by phytochrome, which becomes obvious in the phenotype of *cpm1*, *cpm2* and *hebiba* (Biswas *et al.*, 2003; Riemann *et al.*, 2003; Haga and Iino, 2004; present work), it is an intriguing possibility that phyB regulation of florigen expression is mediated by jasmonate. This possibility warrants further study on the function of jasmonate in the regulation of heading time.

Both *cpm2* and *hebiba* develop long coleoptiles under continuous red light (Figure 1), although the phenotype is more severe in *hebiba* compared to *cpm2.* While *cpm2* is a specific *OsAOC* mutant with a deletion of 11 bp in the first exon, a 170 kb region is missing in *hebiba*, which includes *OsAOC* and other genes. A possibility that explains the difference in severity of phenotypes of these mutants is that *hebiba* is a complete loss-of-function mutant, while *cpm2* produces a truncated, partially functional enzyme. However, this possibility is unlikely because both mutants are similarly incapable of synthesizing JA (Figure 5). Therefore, it is more likely that the difference in phenotype is caused by other genes deleted in *hebiba* (Table S2). One or more of those genes may mediate jasmonate-dependent growth inhibition. As the phenotypes of *hebiba* were complemented well using the *OsAOC* gene, the contribution of such genes may be minor.

Jasmonate mediates resistance to *M. oryzae*

The role played by jasmonate in the response to *M. oryzae* is under debate. It has been reported that the levels of JA and JA–Ile increase after blast infection of intact rice plants (Wakuta *et al.*, 2011; Peng *et al.*, 2012). However, Yara *et al.* (2008) did not find any clear change in blast susceptibility in transgenic rice plants in which expression of *OsAOC* or *OsOPR7* was suppressed by RNAi.

Using the two jasmonate-deficient mutants *cpm2* and *hebiba*, we were able to demonstrate that fungal hyphae of an incompatible strain of *M. oryzae* grow more easily within the tissue (Figure 7). The results indicate that the jasmonate present in the wild-type mediates at least a part of the defence response to *M. oryzae*. An increase in *M. oryzae* susceptibility of the mutants was observed with an incompatible strain but not with a compatible strain (Figure 7 and Figure S6). This may mean that endogenous jasmonate in the wild-type is not sufficient to defend against virulent, compatible strains, and that a further decrease in jasmonate in the mutants does not result in an apparent increase in infection. On the other hand, we showed that exogenously applied JA increases resistance to the compatible strain. This result suggests that, although not effective, jasmonate-mediated defence signalling also operates in a compatible interaction, although not in an effective manner.

The question is whether or not jasmonate levels are enhanced in leaves of wild-type rice in response to blast infection. Our investigations showed that the levels of JA and JA–Ile increase upon blast infection (see above). We observed blast-induced accumulation of JA–Ile but not free JA (Figure 8). This result suggests that OsJAR1, the rice enzyme catalysing conjugation of JA to Ile (Figure 8), is the primary metabolic target of blast infection. However, the partial disagreement with previous reports warrants further investigation (Yara *et al.*, 2008; Wakuta *et al.*, 2011; Peng *et al.*, 2012).

Blast-induced production of phytoalexins is mediated by jasmonate

Several diterpenoid phytoalexins and a flavonoid phytoalexin, sakuranetin, have been identified in blast-infected rice leaves, with sakuranetin being the most abundant (Kodama *et al.*, 1992; Koga *et al.*, 1995 Grayer and Kokubun, 2001). In fact, phytoalexins have been shown to be induced in rice leaves in response to *M. oryzae* infection (Kodama *et al.*, 1992; Dillon *et al.*, 1997). Furthermore, application of exogenous JA induced accumulation of momilactones and sakuranetin (Rakwal *et al.*, 1996), and expression of naringenin-7–*O*–methyltransferase, a key enzyme of sakuranetin biosynthesis, was also found to be

induced by exogenous JA (Tamogami *et al.*, 1997; Shimizu *et al.*, 2012). These results suggest that blast-induced accumulation of phytoalexins is mediated by jasmonate. However, due to the lack of jasmonate-deficient mutants, it has been difficult to demonstrate whether endogenous jasmonate is involved in blast-induced phytoalexin accumulation.

In this paper, we demonstrate that blast-induced accumulation of sakuranetin and momilactones is impaired in jasmonate-deficient mutants, although accumulation of phytocassanes occurred normally in the mutants (Figure 9). It is notable that the induction of sakuranetin was almost completely abolished in the mutants. The result provides clear genetic evidence for the involvement of jasmonate in blast-induced accumulation of sakuranetin and momilactones. The results also indicate that a jasmonate-independent pathway operates for blast-induced accumulation of phytocassanes and partially for accumulation of momilactones. It is thus plausible that jasmonate-mediated phytoalexin accumulation contributes to the defence against blast fungus infection. Our results encourage further investigation into jasmonate-mediated phytoalexin accumulation as a defence mechanism against pathogenic micro-organisms.

EXPERIMENTAL PROCEDURES

Plant material

A *japonica* type rice, cv. Nihonmasari, was used as wild-type. This is also the genetic background of the mutants *hebiba* (Riemann *et al.*, 2003) and *cpm1* (Biswas *et al.*, 2003). The *cpm2* mutant was isolated from γ–ray-mutagenized M_2 lines of Nihonmasari as described by Biswas *et al.* (2003).

For experiments determining the final coleoptile length, surface-sterilized caryopses were sown on 0.7% agar in clear plastic containers. Seedlings were raised at 25 ± 1°C under continuous red light (2–3 μmol m^{-2} sec^{-1}). For infection experiments, plants were routinely grown in a chamber under long-day conditions (14 h light at 28°C and 10 h dark at 24°C) in hydroponic culture (Tanabe *et al.*, 2006).

Chemicals

[$^2H_2$]–JA was purchased from Tokyo Chemical Industry Co. Ltd (http://www.tcichemicals.com/). [$^{13}C_6$]-JA–Ile was synthesized from (±)–methyl jasmonate (Tokyo Chemical Industry Co. Ltd) and [$^{13}C_6$]-isoleucine (Cambridge Isotope Laboratories Inc., http://www.isotope.com/cil/index.cfm) (Jikumaru *et al.*, 2004). 13(S)–hydroperoxy-9(*Z*),11(*E*),15(*Z*)-octadecatrienoic acid (13–HPOT), *cis*-(+)–OPDA and racemic OPDA were purchased from Larodan Fine Chemicals (http://www.larodan.se/), and (±)–JA was purchase from Sigma–Aldrich (http://www.sigmaaldrich.com).

Map-based cloning

cpm2 and *hebiba* were crossed with the *indica* cultivars Kasalath and Habataki, respectively. F_2 seedlings obtained from the cross between *cpm2* and Habataki were incubated under red light and selected for the long-coleoptile phenotype (Figure S1). Genomic DNA was extracted from selected plants (738) by a cetyltrimethylammonium bromide method (Sambrook *et al.*, 1989) and analysed by PCR using SSR markers (International Rice Genome Sequencing Project, 2005). Additional SSR markers for fine mapping were created based on the genomic sequence differences between *japonica* and *indica* rice (Table S1). F_2 seedlings obtained from the cross between *hebiba* and Kasalath were raised under continuous far-red light (Riemann *et al.*, 2008), and individuals with long coleoptiles were selected. SSR markers (Table S1) were applied to narrow down the genomic region deleted in *hebiba*. By inverse PCR, a product of 1800 bp was obtained using the primers 5′-TGGTGAATCATCTCTCATTTGAAATTCC-3′ and 5′-CCTCATGCCACATAGAAGGATC-3′. Subsequently, the flanking border sequences of *hebiba* were amplified directly from genomic *hebiba* DNA by PCR using the primers 5′-GGCGGGGTTAAATCTAGAGG-3′ and 5′-CCTCATGCCACATAGAAGGATC-3′.

Complementation

cpm2 and *hebiba* were transformed with a genomic fragment containing *OsAOC* and a region 2854 bp upstream of the start codon (primer sequences: 5′-GCAAGCTTCAAGAACACACCATAAACGCTCTCC-3′ and 5′-GCGGTACCAACATACACATGGACATGAGCTGGA-3′). The genomic region was cloned into pIG121–Hm–8 (http://lifesciencedb.jp/ddbj-e/card.cgi?project_id=725283) via *Hin*dIII and *Kpn*I. The mutants were transformed with this plasmid using *Agrobacterium*. For each mutant, several lines of the T_1 generation were assayed using the following approach. Caryopses were germinated under continuous red light. The final coleoptile length of each individual was recorded before transplantation into soil. Genomic DNA was extracted to examine the presence of the transgene and the mutation using the primers 5′-GCCTGACCTATTGCATCTCC-3′ and 5′- TACACAGCCATCGGTCCAGA-3′ for the transgene and 5′-ACGAACATCTCCTGCACCTT-3′ and 5′-CTCGCGAGTCTCCGTCAG-3′ for the *cpm2* mutation. Analysis was performed by electrophoresis on a 4% agarose gel (NuSieve agarose, Lonza, http://www.lonza.com/). The presence of the *hebiba* mutation was examined by PCR using the primers 5′-CATGCCACATAGAAGGATC-3′ and 5′-GGCGGGGTTAAATCTAGAGG-3′. For *cpm2* complementation, two selected T_2 lines were assayed as described for the T_1 generation. Additionally, the fertility of each plant was examined by counting empty flowers and flowers containing caryopses.

Expression and purification of GST fusion proteins

A partial sequence of *OsAOC* lacking the chloroplast transit peptide was amplified from Nihonmasari cDNA using Phusion DNA polymerase (Finnzymes, http://www.thermoscientificbio.com/finnzymes/) and the primers 5′-GGATCCTCGCTGTTCTCGCCGAA-3′ and 5′- CTCGAGGCACATGCCGCAATTAACACTA-3′. The PCR product was cloned into pGEX–6P–1 (GE Healthcare, http://www3.gehealthcare.com/en/Global_Gateway) using *Bam*HI and *Xho*I (New England Biolabs, https://www.neb.com/). Competent BL21 *Escherichia coli* were transformed with either pGEX–6–P1 plasmid containing *OsAOC* or *OsAOS1* (K.H. and M.I. unpublished results).

For expression of GST–OsAOS1, the cells were cultivated in Luria–Bertani (LB) medium until an absorbance at 600 nm of 0.75–0.85 prior to induction of protein expression by isopropyl thio-β–D–galactoside (0.1 mM). To express GST–OsAOC, the culture medium was supplemented with isopropyl thio-β–D–galactoside (0.5 mM) directly. Both cultures were incubated for 2 days (18°C, 200 rounds per minute). The culture medium was removed by centrifugation (10 000 ***g***, 4°C, 10 min) and resuspended in 50 mM Tris (pH 7.8) containing 300 mM NaCl, 100 mg/L^{-1} cholic acid, 5 mM

EDTA and 10 mM dithiothreitol. The sedimented cells were suspended in fesh buffer for wahsing and centrifuged (10 000 ***g***, 4°C, 10 min). The supernatant was removed and the cells were suspended in lysis buffer (50 mM Tris (pH 7.8), 300 mM NaCl, 100 mg mL^{-1} cholic acid, 5 mM EDTA and 10 mM DTT). After an incubation of 1 hour on ice cells were disrupted in a French pressure cell, and centrifuged (20 000 ***g***, 4°C, 40 min). The proteins were precipitated by addition of an equal volume of 3.3 M ammonium sulfate containing 50 mM Tris (pH 7.8). This suspension was centrifuged (20 000 ***g***, 4°C, 10 min) and the sediment was resuspended in phosphate-buffered saline. Subsequently, the GST fusion proteins were purified using glutathione Sepharose 4B (GE Healthcare) according to the manufacturer's instruction. Fractions of purified proteins were analysed by SDS–PAGE and Coomassie staining (Figure S2).

Coupled enzyme activity assay

The enzyme reaction for OsAOC was performed as described by Stenzel *et al.* (2003) with minor modifications. Affinity-purified GST–OsAOS1 (10 μg) and GST–OsAOC (30 μg) were incubated with 25 μM of 13–HPOT in 50 mM sodium phosphate buffer (pH 7, 25°C, 1 h). Subsequently, the reaction products were extracted with two volumes of ethyl acetate, and subjected to capillary GC–MS after treatment with ethereal diazomethane. The enantiomer preference of OsAOC was examined by chiral GC–MS using a JMS–Q1000 K9 system (JEOL, http://www.jeol.com/), fitted with a wall-coated open tubular column fused-silica chemically bonded capillary Chirasil–DEX column (length 10 m, 0.25 mm internal diameter, 0.25 μm thick; Varian, www.varianinc.com). The identification of reaction products was performed as described previously (Tani *et al.*, 2008).

Extraction and determination of jasmonates

Plant tissues (40–200 mg FW) were homogenized with a Multi Beads Shocker (Yasui Kikai Corporation, http://www.yasuikikai.co.jp/) and suspended in 2 ml of 80% v/v methanol containing 1% v/v acetic acid. After addition of 10 ng $[^2H_2]$-JA and $[^{13}C_6]$-JA–Ile, the suspension was centrifuged (15 min, 4°C, 8000 ***g***). The supernatant was loaded onto a Sep–Pak C_{18} cartridge (500 mg, 3 ml; Waters) and eluted using 3 ml of 80% v/v methanol containing 1% v/v acetic acid. The cartridge was pre-washed with 3 ml each of methanol and water after equilibration with 3 ml of 80% v/v methanol containing 1% v/v acetic acid. The flow-through and eluted fractions were combined together and concentrated to approximately 1 ml *in vacuo*. This sample was loaded onto an Oasis MAX cartridge (150 mg, 3 ml; Waters), and washed (25°C) sequentially using 3 ml of 50 mM KH_2PO_4 (pH 8.0), water, methanol, water, water containing 1% v/v acetic acid, and 30% v/v methanol containing 1% v/v acetic acid. It was then eluted with 3 ml of 80% v/v methanol containing 1% v/v acetic acid. Before sample loading, the cartridge was pre-washed with 3 ml each methanol and water, and equilibrated with 3 ml of water containing 1% v/v acetic acid. The eluate was concentrated to approximately 1 ml *in vacuo*. The concentrated sample was subjected to LC-ESI-MS/MS, comprising a quadrupole tandem mass spectrometer (API–3000, AB Sciex, http://www.absciex.com/) with an electrospray ion source and an Agilent 1100 HPLC instrument (Agilent Technologies, http://www.home.agilent.com) equipped with a PEGASIL ODS column (length 150 mm, internal diameter 2 mm; Senshu Scientific Co. Ltd, http://www.ssc-jp.com/) or a Sumichiral OA–7500 column (length 250 mm, diameter 2 mm; Sumika Chemical Analysis Service, http://www.scas.co.jp/). The solvents used for both columns were water (A) and acetonitrile containing 0.1% v/v acetic acid (B). A 20 min linear gradient (5–100% B) was applied 5 min after sample injection (flow rate 0.2 ml min^{-1}). Multiple reaction monitoring (MRM) mode was used in ESI-MS/MS to monitor precursors and products. JA and JA–Ile were analysed in negative-ion mode with nitrogen as the collision gas. JA, $[^2H_2]$-JA, JA–Ile and $[^{13}C_6]$-JA–Ile were determined of *m/z* 209/59, *m/z* 211/59, *m/z* 322/130 and *m/z* 328/136, respectively.

Preparation of fungal conidia

Blast fungi causing an incompatible (*M. oryzae* P91–15B, race 001.0) or compatible (*M. oryzae* Ina86–137, race 007.0) interaction were grown on 60 g l^{-1} homogenized oatmeal and 12 g l^{-1} agar in Petri dishes (25°C, 9 days). Conidial suspension was prepared as described by Koga (1994), and filtered through two layers of Miracloth (Calbiochem, http://www.merckgroup.com/en/index.html) to remove cell debris. The conidial suspension was used for inoculation tests within 2 h after preparation.

Fungal inoculation

The fourth leaf sheaths in the 4.5-leaf stage (3–4 weeks) were excised and inoculated with a conidial suspension (concentration 10^5 spores ml^{-1}) and incubated in darkness (25°C, 48 h). After fixation in a solution containing 5% v/v formaldehyde, 5% v/v acetic acid and 45% v/v ethanol, the level of infection was determined microscopically by counting appressoria. The extent of infection was separated into three categories: 'infected' (more than one cell was infected with hyphae originating from the observed appressorium), 'one cell infected' (only one cell beneath the observed appressorium was infected by hyphae) or 'non-infected' (no cell was infected by the observed appressorium), as described by Tanabe *et al.* (2006). To supplement the hydroponic culture medium with exogenous JA, (±)–JA was added (final concentration 100 μM) 24 h before inoculation.

Extraction and determination of phytoalexins

Plant tissue (40–200 mg FW) was homogenized using a Multi Beads Shocker and suspended in 2 ml of 80% v/v methanol containing 1% v/v acetic acid. The sample was centrifuged (4°C, 15 min, 800 ***g***). The supernatant was collected and subjected to phytoalexin analysis by LC-ESI-MS/MS, comprising an API-3000 spectrometer with an electrospray ion source and an Agilent 1100 HPLC instrument equipped with a Pegasil ODS column (Shimizu *et al.*, 2008). Phytoalexin levels were determined using combinations of precursor and product ions (*m/z* 317/299 for phytocassanes A, D and E; *m/z* 335/317 for phytocassane B; *m/z* 315/271 for phytocassane C; *m/z* 315/271 for momilactone A; *m/z* 331/269 for momilactone B; *m/z* 287/167 for sakuranetin) in MRM mode. The retention times (in min) for phytocassanes A, B, C, D and E, momilactones A and B, and sakuranetin were 4.8, 4.2, 3.8, 5.9, 5.3, 6.4, 4.9 and 3.3, respectively.

ACKNOWLEDGEMENTS

This work was supported by the Japan Society for the Promotion of Science (KAKENHI grant number 16370027) and the Ministry of Education, Culture, Sports, Science and Technology (KAKENHI grant number 23120524) to M.I., and by the Programme for Promotion of Basic and Applied Researches for Innovations in Bio-oriented Industry to K.O. and H.Y. T.S. was supported by the Japan Society for the Promotion of Science as a research fellow. M.R. was supported by a postdoctoral fellowship from the Japan Society for the Promotion of Science and the Alexander von Humboldt Foundation. We would like to thank Y. Iguchi and Y. Mitsubayashi for technical assistance.

SUPPORTING INFORMATION

Additional Supporting Information may be found in the online version of this article.

Figure S1. Segregation of the long-coleoptile phenotype in the F_2 mapping population.

Figure S2. Coomassie staining of affinity-purified GST–OsAOS1 and GST–OsAOC.

Figure S3. Cyclization of allene oxide to (+)–*cis*-OPDA by OsAOC.

Figure S4. Effect of wounding on accumulation of jasmonates in leaf blades.

Figure S5. Impaired husk closure in *cpm2* and *hebiba*.

Figure S6. *Magnaporthe oryzae* (Ina86–137) inoculation assay with excised leaf sheaths.

Figure S7. Effect of fungal inoculation on accumulation of each component of the major diterpenoid phytoalexins of rice in wild-type, *cpm2* and *hebiba*.

Table S1. Primer sequences of SSR markers.

Table S2. Genes deleted in *hebiba*.

REFERENCES

Acosta, I.F., Laparra, H., Romero, S.P., Schmelz, E., Hamberg, M., Mottinger, J.P., Moreno, M.A. and Dellaporta, S.L. (2009) *tasselseed1* is a lipoxygenase affecting jasmonic acid signaling in sex determination of maize. *Science*, **323**, 262–265.

Biswas, K.K., Neumann, R., Haga, K., Yatoh, O. and Iino, M. (2003) Photomorphogenesis of rice seedlings: a mutant impaired in phytochrome-mediated inhibition of coleoptile growth. *Plant Cell Physiol.* **44**, 242–254.

Bottcher, C. and Pollmann, S. (2009) Plant oxylipins: plant responses to 12–oxo-phytodienoic acid are governed by its specific structural and functional properties. *FEBS J.* **276**, 4693–4704.

Chen, I.–C., Huang, I.C., Liu, M.–J., Wang, Z.–G., Chung, S.–S. and Hsieh, H.–L. (2007) Glutathione *S*–transferase interacting with far-red insensitive 219 is involved in phytochrome A-mediated signaling in Arabidopsis. *Plant Physiol.* **143**, 1189–1202.

Chi, M.H., Park, S.–Y., Kim, S. and Lee, Y.H. (2009) A novel pathogenicity gene is required in the rice blast fungus to suppress the basal defenses of the host. *PLoS Pathog.* **5**, e1000401.

Chini, A., Fonseca, S., Fernandez, G. *et al.* (2007) The JAZ family of repressors is the missing link in jasmonate signalling. *Nature*, **448**, 666–671.

Dillon, V.M., Overton, J., Grayer, R.J. and Harborne, J.B. (1997) Differences in phytoalexin response among rice cultivars of different resistance to blast. *Phytochemistry*, **44**, 599–603.

Falkenstein, E., Groth, B., Mithofer, A. and Weiler, E.W. (1991) Methyljasmonate and alpha-linolenic acid are potent inducers of tendril coiling. *Planta*, **185**, 316–322.

Grayer, R.J. and Kokubun, T. (2001) Plant–fungal interactions: the search for phytoalexins and other antifungal compounds from higher plants. *Phytochemistry*, **56**, 253–263.

Haga, K. and Iino, M. (2004) Phytochrome-mediated transcriptional up-regulation of allene oxide synthase in rice seedlings. *Plant Cell Physiol.*, **45**, 119–128.

Hamberg, M. and Fahlstadius, P. (1990) Allene oxide cyclase: a new enzyme in plant lipid metabolism. *Arch. Biochem. Biophys.*, **276**, 518–526.

Hsieh, H.–L., Okamoto, H., Wang, M., Ang, L.–H., Matsui, M., Goodman, H. and Deng, X.W. (2000) *FIN219*, an auxin-regulated gene, defines a link between phytochrome A and the downstream regulator COP1 in light control of Arabidopsis development. *Genes Dev.*, **14**, 1958–1970.

International Rice Genome Sequencing Project (2005) The map-based sequence of the rice genome. *Nature*, **436**, 793–800.

Ishiguro, S., Kawai-Oda, A., Ueda, J., Nishida, I. and Okada, K. (2001) The *DEFECTIVE IN ANTHER DEHISCIENCE* gene encodes a novel phospholipase A1 catalyzing the initial step of jasmonic acid biosynthesis, which synchronizes pollen maturation, anther dehiscence, and flower opening in Arabidopsis. *Plant Cell*, **13**, 2191–2209.

Ishikawa, R., Aoki, M., Kurotani, K., Yokoi, S., Shinomura, T., Takano, M. and Shimamoto, K. (2011) Phytochrome B regulates *Heading date 1* (*Hd1*)-mediated expression of rice florigen *Hd3a* and critical day length in rice. *Mol. Genet. Genomics*, **285**, 461–470.

Izawa, T., Oikawa, T., Sugiyama, N., Tanisaka, T., Yano, M. and Shimamoto, K. (2002) Phytochrome mediates the external light signal to repress FT orthologs in photoperiodic flowering of rice. *Genes Dev.*, **16**, 2006–2020.

Jikumaru, Y., Asami, T., Seto, H. *et al.* (2004) Preparation and biological activity of molecular probes to identify and analyze jasmonic acid-binding proteins. *Biosci. Biotechnol. Biochem.*, **68**, 1461–1466.

Kiribuchi, K., Jikumaru, Y., Kaku, H., Minami, E., Hasegawa, M., Kodama, O., Seto, H., Okada, K., Nojiri, H. and Yamane, H. (2005) Involvement of the basic helix-loop-helix transcription factor RERJ1 in wounding and drought stress responses in rice plants. *Biosci. Biotechnol. Biochem.*, **69**, 1042–1044.

Kodama, O., Miyakawa, J., Akatsuka, T. and Kiyosawa, S. (1992) Sakuranetin, a flavanone phytoalexin from ultraviolet-irradiated rice leaves. *Phytochemistry*, **31**, 3807–3809.

Koga, H. (1994) Hypersensitive death, autofluorescence and ultrastructural changes in cells of leaf sheaths of susceptible and resistant near-isogenic lines of rice (Pi–z–t) in relation to penetration and growth of *Pyricularia oryzae*. *Can. J. Bot.*, **72**, 1463–1477.

Koga, J., Shimura, M., Oshima, K., Ogawa, N., Yamauchi, T. and Ogasawara, N. (1995) Phytocassanes A, B, C and D, novel diterpene phytoalexins from rice, *Oryza sativa* L. *Tetrahedron*, **51**, 7907–7918.

Koo, A.J. and Howe, G.A. (2009) The wound hormone jasmonate. *Phytochemistry*, **70**, 1571–1580.

Nicholson, R.L., Kollipara, S.S., Vincent, J.R., Lyons, P.C. and Cadena-Gomez, G. (1987) Phytoalexin synthesis by the sorghum mesocotyl in response to infection by pathogenic and nonpathogenic fungi. *Proc. Natl Acad. Sci. USA*, **84**, 5520–5524.

Nordström, K.J.V., Albani, M.C., James, G.V., Gutjahr, C., Hartwig, B., Turck, F., Paszkowski, U., Coupland, G. and Schneeberger, K. (2013) Mutation identification by direct comparison of whole-genome sequencing data from mutant and wild-type individuals using k-mers. *Nature Biotech.*, doi: 10.1038/nbt.2515.

Peng, X., Hu, Y., Tang, X., Zhou, P., Deng, X., Wang, H. and Guo, Z. (2012) Constitutive expression of rice *WRKY30* gene increases the endogenous jasmonic acid accumulation, *PR* gene expression and resistance to fungal pathogens in rice. *Planta*, **236**, 1485–1498.

Pu, C.X., Ma, Y., Wang, J., Zhang, Y.C., Jiao, X.W., Hu, Y.H, Wang, L.L., Zhu, Z.G., Sun, D. and Sun, Y. (2012) Crinkly4 receptor-like kinase is required to maintain the interlocking of the palea and lemma, and fertility in rice, by promoting epidermal cell differentiation. *Plant J.*, **70**, 940–953.

Rakwal, R., Tamogami, S. and Kodama, O. (1996) Role of jasmonic acid as a signaling molecule in copper chloride-elicited rice phytoalexin production. *Biosci. Biotechnol. Biochem.*, **60**, 1046–1048.

Reinbothe, C., Springer, A., Samol, I. and Reinbothe, S. (2009) Plant oxylipins: role of jasmonic acid during programmed cell death, defence and leaf senescence. *FEBS J.*, **276**, 4666–4681.

Riemann, M., Muller, A., Korte, A., Furuya, M., Weiler, E.W. and Nick, P. (2003) Impaired induction of the jasmonate pathway in the rice mutant *hebiba*. *Plant Physiol.*, **133**, 1820–1830.

Riemann, M., Gutjahr, C., Korte, A., Danger, B., Muramatsu, T., Bayer, U., Waller, F., Furuya, M. and Nick, P. (2007) GER1, a GDSL motif-encoding gene from rice is a novel early light- and jasmonate-induced gene. *Plant Biol.*, **9**, 32–40.

Riemann, M., Riemann, M. and Takano, M. (2008) Rice JASMONATE RESISTANT 1 is involved in phytochrome and jasmonate signalling. *Plant, Cell Environ.*, **31**, 783–792.

Riemann, M., Bouyer, D., Hisada, A., Müller, A., Yatou, O., Weiler, E.W., Takano, M., Furuya, M. and Nick, P. (2009) Phytochrome A requires jasmonate for photodestruction. *Planta*, **229**, 1035–1045.

Robson, F., Okamoto, H., Patrick, E., Harris, S.R., Wasternack, C., Brearley, C. and Turner, J.G. (2010) Jasmonate and phytochrome A signaling in Arabidopsis wound and shade responses are integrated through JAZ1 stability. *Plant Cell*, **22**, 1143–1160.

Sambrook, J., Fritsch, E.F. and Maniatis, T. (1989) *Molecular Cloning: A Laboratory Manual*, 2nd edn. Cold Spring Harbor: Cold Spring Harbor Laboratory Press.

Schweizer, P., Buchala, A. and Metraux, J.P. (1997) Gene-expression patterns and levels of jasmonic acid in rice treated with the resistance inducer 2,6–dichloroisonicotinic acid. *Plant Physiol.*, **115**, 61–70.

Shimizu, T., Jikumaru, Y., Okada, A. *et al.* (2008) Effects of a bile acid elicitor, cholic acid, on the biosynthesis of diterpenoid phytoalexins in suspension-cultured rice cells. *Phytochemistry*, **69**, 973–981.

Shimizu, T., Lin, F., Hasegawa, M., Okada, K., Nojiri, H. and Yamane, H. (2012) Purification and identification of naringenin 7–*O*–methyltransferase, a key enzyme in the biosynthesis of the flavonoid phytoalexin sakuranetin in rice. *J. Biol. Chem.*, **287**, 19315–19325.

Staswick, P.E. (2008) JAZing up jasmonate signaling. *Trends Plant Sci.*, **13**, 66–71.

Staswick, P.E. and Tiryaki, I. (2004) The oxylipin signal jasmonic acid is activated by an enzyme that conjugates it to isoleucine in Arabidopsis. *Plant Cell*, **16**, 2117–2127.

Stenzel, I., Hause, B., Miersch, O., Kurz, T., Maucher, H., Weichert, H., Ziegler, J., Feussner, I. and Wasternack, C. (2003) Jasmonate biosynthesis and the allene oxide cyclase family of *Arabidopsis thaliana*. *Plant Mol. Biol.*, **51**, 895–911.

Stintzi, A., Weber, H., Reymond, P., Browse, J. and Farmer, E.E. (2001) Plant defense in the absence of jasmonic acid: the role of cyclopentenones. *Proc. Natl Acad. Sci. USA*, **98**, 12837–12842.

Takano, M., Inagaki, N., Xie, X. ***et al.*** (2005) Distinct and cooperative functions of phytochromes A, B, and C in the control of deetiolation and flowering in rice. *Plant Cell*, **17**, 3311–3325.

Taki, N., Sasaki-Sekimoto, Y., Obayashi, T. ***et al.*** (2005) 12-oxo–phytodienoic acid triggers expression of a distinct set of genes and plays a role in wound-induced gene expression in Arabidopsis. *Plant Physiol.*, **139**, 1268–1283.

Tamaki, S., Matsuo, S., Wong, H.L., Yokoi, S. and Shimamoto, K. (2007) Hd3a protein is the mobile flowering signal in rice. *Science*, **316**, 1033–1036.

Tamogami, S., Rakwal, R. and Kodama, O. (1997) Phytoalexin production by amino acid conjugates of jasmonic acid through induction of naringenin-7–*O*–methyltransferase, a key enzyme on phytoalexin biosynthesis in rice (*Oryza sativa* L.). *FEBS Lett.* **401**, 239–242.

Tanabe, S., Okada, M., Jikumaru, Y., Yamane, H., Kaku, H., Shibuya, N. and Minami, E. (2006) Induction of resistance against rice blast fungus in rice plants treated with a potent elicitor, *N*–acetylchitooligosaccharide. *Biosci. Biotechnol. Biochem.*, **70**, 1599–1605.

Tani, T., Sobajima, H., Okada, K., Chujo, T., Arimura, S., Tsutsumi, N., Nishimura, M., Seto, H., Nojiri, H. and Yamane, H. (2008) Identification of the *OsOPR7* gene encoding 12–oxophytodienoate reductase involved in the biosynthesis of jasmonic acid in rice. *Planta*, **227**, 517–526.

Thines, B., Katsir, L., Melotto, M., Niu, Y., Mandaokar, A., Liu, G., Nomura, K., He, S.Y., Howe, G.A. and Browse, J. (2007) JAZ repressor proteins are targets of the SCFCO11 complex during jasmonate signalling. *Nature*, **448**, 661–665.

Vick, B.A. and Zimmerman, D.C. (1984) Biosynthesis of jasmonic-acid by several plant species. *Plant Physiol.* **75**, 458–461.

Wakuta, S., Suzuki, E., Saburi, W., Matsuura, H., Nabeta, K., Imai, R. and Matsui, H. (2011) OsJAR1 and OsJAR2 are jasmonyl-L–isoleucine synthases involved in wound- and pathogen-induced jasmonic acid signalling. *Biochem. Biophys. Res. Commun.* **409**, 634–639.

Wasternack, C. (2007) Jasmonates: an update on biosynthesis, signal transduction and action in plant stress response, growth and development. *Ann. Bot.* **100**, 681–697.

Xie, D.X., Feys, B.F., James, S., Nieto-Rostro, M. and Turner, J.G. (1998) *COI1*: an Arabidopsis gene required for jasmonate-regulated defense and fertility. *Science*, **280**, 1091–1094.

Yan, Y., Christensen, S., Isakeit, T., Engelberth, J., Meeley, R., Hayward, A., Emery, R.J. and Kolomiets, M.V. (2012) Disruption of *OPR7* and *OPR8* reveals the versatile functions of jasmonic acid in maize development and defense. *Plant Cell*, **24**, 1420–1436.

Yang, D.L., Yao, J., Mei, C.S. ***et al.*** (2012) Plant hormone jasmonate prioritizes defense over growth by interfering with gibberellin signaling cascade. *Proc. Natl Acad. Sci. USA*, **109**, E1192–E1200.

Yara, A., Yaeno, T., Hasegawa, M., Seto, H., Seo, S., Kusumi, K. and Iba, K. (2008) Resistance to *Magnaporthe grisea* in transgenic rice with suppressed expression of genes encoding allene oxide cyclase and phytodienoic acid reductase. *Biochem. Biophys. Res. Commun.* **376**, 460–465.

Yoshida, H. and Nagato, Y. (2011) Flower development in rice. *J. Exp. Bot.*, **62**, 4719–4730.

Zerbe, P., Weiler, E.W. and Schaller, F. (2007) Preparative enzymatic solid phase synthesis of *cis*(+)-12–oxo-phytodienoic acid – physical interaction of AOS and AOC is not necessary. *Phytochemistry*, **68**, 229–236.